© 2018. Published by The Company of Biologists Ltd | Journal of Cell Science (2018) 131, jcs210724. doi:10.1242/jcs.210724

RESEARCH ARTICLE

Acute HSF1 depletion induces cellular senescence through the MDM2-p53-p21 pathway in human diploid fibroblasts

Tsukasa Oda[1], Takayuki Sekimoto[1], Kiminori Kurashima[1], Mitsuaki Fujimoto[2], Akira Nakai[2] and Takayuki Yamashita[1,*]

ABSTRACT

Heat shock transcription factor 1 (HSF1) regulates the expression of a wide array of genes, controls the expression of heat shock proteins (HSPs) as well as cell growth. Although acute depletion of HSF1 induces cellular senescence, the underlying mechanisms are poorly understood. Here, we report that HSF1 depletion-induced senescence (HDIS) of human diploid fibroblasts (HDFs) was independent of HSP-mediated proteostasis but dependent on activation of the p53-p21 pathway, partly because of the increased expression of dehydrogenase/reductase 2 (DHRS2), a putative MDM2 inhibitor. We observed that HDIS occurred without decreased levels of major HSPs or increased proteotoxic stress in HDFs. Additionally, VER155008, an inhibitor of HSP70 family proteins, increased proteotoxicity and suppressed cell growth but failed to induce senescence. Importantly, we found that activation of the p53-p21 pathway resulting from reduced MDM2-dependent p53 degradation was required for HDIS. Furthermore, we provide evidence that increased DHRS2 expression contributes to p53 stabilization and HDIS. Collectively, our observations uncovered a molecular pathway in which HSF1 depletion-induced DHRS2 expression leads to activation of the MDM2-p53-p21 pathway required for HDIS.

KEY WORDS: Cellular senescence, HSF1, p53 (TP53), MDM2, DHRS2

INTRODUCTION

Cellular senescence is a complex process wherein cells permanently exit the cell cycle in response to various stresses (Campisi, 2013; He and Sharpless, 2017; Muñoz-Espín and Serrano, 2014). Other hallmarks of senescent cells include increased activity of the lysosomal enzyme senescence-associated β-galactosidase (SA-β-gal; also known as GLB1), formation of senescence-associated heterochromatin foci (SAHF), expression of tumor suppressor and cell cycle regulatory proteins, such as p53 (officially known as TP53) and p21 (CDKN1A), and secretion of inflammatory cytokines and matrix-degrading proteases, which taken together are termed senescence-associated secretory phenotype (SASP). Cellular senescence serves as an important anti-cancer barrier by linking oncogenic signals to the activation of tumor suppressor pathways (Campisi, 2013; He and Sharpless, 2017; Muñoz-Espín and Serrano, 2014). In addition, increasing evidence indicates that senescent cells contribute to the expression of various aging-related phenotypes (Baker et al., 2016, 2011). These effects are mainly mediated by growth arrest of tissue progenitor cells and paracrine actions of SASP.

Heat shock transcription factor 1 (HSF1) plays a central role in protein homeostasis by transcriptionally activating the expression of heat shock proteins (HSPs) (Anckar and Sistonen, 2011; Gomez-Pastor et al., 2017; Labbadia and Morimoto, 2015). Additionally, HSF1 regulates the expression of various genes encoding important regulators of cell growth, survival and metabolism (Hahn et al., 2004; Mendillo et al., 2012; Takii et al., 2015). While the most prominent phenotype of HSF1-deficient organisms is the development of aging-related neurodegenerative disorders, mainly caused by accumulation of aggregates from misfolded proteins (Anckar and Sistonen, 2011; Gomez-Pastor et al., 2017; Labbadia and Morimoto, 2015), the mechanisms underlying multiple abnormalities, such as developmental defects and increased expression of inflammatory cytokines, remain to be clarified. Another remarkable phenotype of HSF1-deficient mice models is the suppression of tumor development (Dai et al., 2007; Min et al., 2007). One interesting hypothesis is that some of these phenotypes of HSF1-deficient organisms are based on cellular senescence. Indeed, Sherman and colleagues have reported that the downregulation of HSF1 induces cellular senescence in transformed human epithelial cells and normal human diploid fibroblasts (HDFs) (Kim et al., 2012; Meng et al., 2010). These studies have demonstrated that increased levels of p21 and decreased levels of HSPs are associated with HSF1 depletion-induced cellular senescence (HDIS). However, the molecular mechanisms of this process are poorly characterized. Specifically, the signaling pathway upstream of p21, including the involvement of p53 activation and increased proteotoxic stress, has not been fully studied.

To address these issues, we produced immortalized HDFs in which drug-induced expression of short hairpin RNA (shRNA) targeting the non-coding region of the *HSF1* gene induces cellular senescence. Using this experimental system, we obtained evidence that, unlike the commonly accepted notion, HSF1 depletion induces cellular senescence without reduced expression of HSPs and increased proteotoxic stress. We also demonstrated that activation of the MDM2-p53-p21 pathway was required for HDIS. Furthermore, we found that this pathway activation was mediated in part by the increased expression of dehydrogenase/reductase 2 (DHRS2), a putative MDM2 inhibitor (Deisenroth et al., 2010). The present findings provide previously unknown mechanistic insight into the regulatory role of HSF1 in cellular senescence.

[1]Laboratory of Molecular Genetics, The Institute for Molecular and Cellular Regulation, Gunma University, Maebashi, Gunma 371-8512, Japan. [2]Department of Biochemistry and Molecular Biology, Yamaguchi University School of Medicine, Ube, Yamaguchi 755-8505, Japan.

*Author for correspondence (y-taka@gunma-u.ac.jp)

T.Y., 0000-0003-2074-9310

Received 8 September 2017; Accepted 3 April 2018

Journal of Cell Science (2018) 131, jcs210724. doi:10.1242/jcs.210724

RESULTS

RNA interference (RNAi)-mediated HSF1 depletion induces cellular senescence in non-transformed HDFs

Kim et al. have previously reported that shRNA-mediated depletion of HSF1 induced cellular senescence in the normal HDF cell line TIG-1 (Kim et al., 2012). We asked whether this effect is reproducible in other normal HDF lines and human telomerase reverse transcriptase (hTERT)-immortalized HDFs. Introduction of a lentiviral vector expressing shRNA targeting the 3′-untranslated region (UTR) of *HSF1* (shHSF1) to the normal HDF cell line MRC-5, depleted HSF1 and resulted in various phenotypes characteristic of cellular senescence – including growth arrest and suppression of DNA synthesis, and the appearance of enlarged cells positive for SA-β-gal and SAHF (Fig. S1A-E). Similar effects of HSF1 depletion were observed in the normal HDF lines TIG-1 and TIG-3, and in the hTERT-immortalized HDF line OUMS-36T-3F (Fig. S1F-H). The expression of shHSF1 targeting a different region of HSF1 (shHSF1 #2) also induced SA-β-gal in OUMS-36T-3F cells (Fig. S1H). By contrast, shRNA-mediated depletion of HSF2, which is known to modulate HSF1-induced gene expression (Östling et al., 2007), failed to increase the number of SA-β-gal-positive cells (Fig. S1H). Collectively, these data indicate that acute depletion of HSF1 specifically induces cellular senescence in several types of non-transformed HDF.

To study the molecular mechanisms of HDIS, we produced OUMS-36T-3F cells expressing doxycycline (DOX)-inducible shHSF1 (OUMS/Tet-on shHSF1). DOX treatment of these cells suppressed HSF1 levels and cell growth, and induced a progressive decrease in DNA synthesis from 48 h to 15 days (Fig. 1A–C). Concurrently, this treatment increased the percentages of SA-β-gal-positive cells and SAHF-positive cells to ∼30% (Fig. 1D,E; Fig. S1I, J). Flow cytometry analysis also showed that ∼30% of cells (fraction F2 in Fig. 1F) exhibited typical senescent morphology, increased forward scatter (FSC) and side scatter (SSC) (measurements of cell size and internal complexity of a cell, respectively), as reported previously (Sugrue et al., 1997). Cells in fraction F2 were arrested in G1 and G2 phases, whereas cells in fraction F1 of the DOX-treated cultures accumulated in G1 phase, potentially reflecting a pro-senescent state (Fig. 1F). In addition, 7 days after treatment, DOX-treated cells exhibited increased mRNA levels of interleukin 6 (*IL6*), C-C motif chemokine ligand 2 (*CCL2*), C-X-C motif chemokine ligand 11 (*CXCL11*) and transforming growth factor β-2 (*TGFB2*), all of which encode proteins present in the SASP (Fig. 1G). Finally, ectopic expression of shHSF1-resistant wild-type (WT) HSF1 in OUMS/Tet-on shHSF1 cells suppressed DOX-induced senescence (Fig. 1H). Thus, OUMS/Tet-on shHSF1 cells provide an experimental system useful for studying the molecular mechanisms of HDIS in non-transformed HDFs.

HDIS is not associated with reduced expression of HSPs or increased proteotoxic stress

Previous studies reported that HSF1 inhibition-induced suppression of cell growth is associated with the reduced expression of HSPs and subsequent increased proteotoxic stress (Kim et al., 2012; Tang et al., 2015). In addition, the depletion of HSPs induced cellular senescence in several tumor cell lines (Gabai et al., 2009; Meng et al., 2011; O'Callaghan-Sunol et al., 2007; Rohde et al., 2005). To elucidate the role of HSP expression in HDIS in OUMS/Tet-on shHSF1 cells, we monitored the expression levels of HSPs during the course of HDIS. However, the protein levels of these HSPs did not significantly change 15 days after DOX treatment (Fig. 2A and Fig. S2A). The protein levels of HSPB5 (αB-crystallin, also known as CRYAB) gradually increased in the HSF1-depleted cells (Fig. 2A and Fig. S2A), suggesting that this increase is a consequence rather than a cause of senescence. To support this notion, HSPB5 expression was also observed during adriamycin-induced senescence of these cells (data not shown). To study the association between HSP expression and cellular senescence at the single cell level, we compared signals of heat shock 70 kDa protein 1A (HSP72, also known as HSPA1A) between SA-β-gal-positive and negative cells (Fig. S2B). The results show that the HSPA1A levels in SA-β-gal-positive cells were similar to those in the SA-β-gal-negative cells, or vehicle-treated cells (Fig. S2B). Collectively, our data indicate that HDIS is not mediated by the decreased expression of HSPs. One possible explanation for the lack of reduced HSP levels in HSF1-depleted cells is that residual amounts of HSF1 are sufficient for the basal expression of HSPs. Alternatively, HSF1 might not be essential for the basal transcription of HSP genes in mammals, as reported by a recent study where the mRNA levels of HSP genes were not reduced in Hsf1-null murine embryonic fibroblasts and stem cells (Solís et al., 2016).

We next studied the association between cellular senescence and increased proteotoxic stress. To assess proteotoxic stress levels, we measured the total amounts of K48-linked polyubiquitylated proteins in the presence of different concentrations of the proteasome inhibitor MG132. While levels of polyubiquitylated proteins were drastically increased upon treatment with the inhibitor of HSP70 family proteins VER155008 (Massey et al., 2010), they did not significantly change in HSF1-depleted cells (Fig. 2B). We also investigated whether increased proteotoxic stress induces cellular senescence in OUMS/Tet-on shHSF1 cells. For this purpose, we treated the cells with VER155008 for 7 days. This treatment suppressed cell growth (Fig. 2C) but failed to induce cellular senescence (Fig. 2D) or activate the p53-p21 pathway (Fig. 2E), which plays a critical role in HDIS, as described in the next section. Collectively, our data indicate that proteotoxic stress is not involved in HDIS of OUMS/Tet-on shHSF1 cells.

HDIS is mediated by activation of the p53-p21 pathway

A previous study reported that p21 mediates HDIS (Meng et al., 2010). Consistent with this, immunostaining analysis showed increased nuclear signals of p21 in almost all DOX-treated OUMS/Tet-on shHSF1 cells (Fig. S3A), indicating that they accumulated in the G1 phase without senescent morphology as described above (Fig. 1F). Because signaling upstream of p21 activation in HDIS remains to be studied, we examined the involvement of p53, the best-known transcription factor of p21 (Abbas and Dutta, 2009; Warfel and El-Deiry, 2013). Immunoblot analysis showed that p53 and p21 protein levels progressively increased in DOX-treated OUMS/Tet-on shHSF1 cells (Fig. 3A). p53 levels were significantly increased 3 days after DOX treatment, whereas p21 levels were increased after 6 days or later. These results are consistent with the notion that p21 induction is dependent on p53 expression.

The increase in p21 protein levels was accompanied by increased mRNA levels of *p21* but not those of *p53* (Fig. S3B), suggesting that *p21* gene expression is transcriptionally activated by p53, whereas p53 expression is regulated at post-transcriptional levels. Further supporting this notion, mRNA levels of other p53 target genes (Ragazzon et al., 2010), including *MDM2*, tumor protein p53-inducible nuclear protein 1 (*TP53INP1*) and ribonucleotide reductase regulatory TP53 inducible subunit M2B (*RRM2B*), were increased (Fig. S3C). The MDM2 protein level increased with a time course similar to that of the p21 protein, as shown by immunoblot analysis (Fig. 3A). Increased p53 and p21 protein levels were also observed in HSF1-depleted MRC-5 and TIG-3 cells

Journal of Cell Science (2018) 131, jcs210724. doi:10.1242/jcs.210724

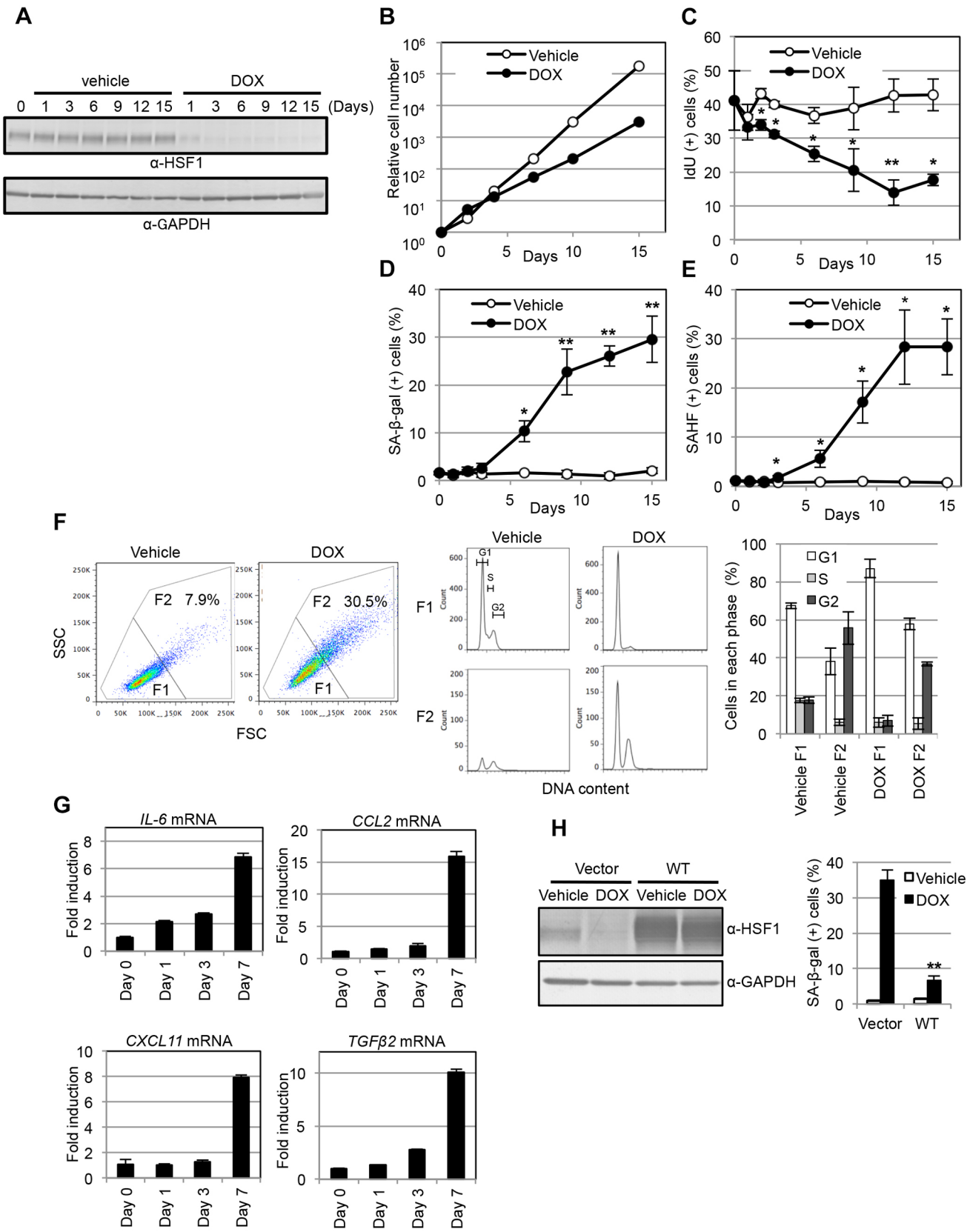

Fig. 1. See next page for legend.

(Fig. S3D). Collectively, these data indicate that p53 is post-transcriptionally upregulated in HSF1-depleted HDFs, which is the most likely cause of the increased expression of *p21*.

To test whether activation of the p53-p21 pathway is required for HDIS, we introduced human papilloma virus type-16 E6 (HPV16 E6), which induces p53 degradation (Duensing and Münger, 2004),

Journal of Cell Science (2018) 131, jcs210724. doi:10.1242/jcs.210724

Fig. 1. RNAi-mediated HSF1-depletion induces cellular senescence in non-transformed HDFs. (A) OUMS/Tet-on shHSF1 cells were treated with vehicle or 1 µg/ml DOX for the indicated times and whole-cell lysates were immunoblotted with the indicated antibodies. (B) OUMS/Tet-on shHSF1 cells were treated with vehicle or DOX for the indicated times. Cells were counted and the relative cell numbers were calculated. Similar results were obtained from three independent experiments. (C) OUMS/Tet-on shHSF1 cells were treated with vehicle or DOX and pulse-labeled with IdU at the indicated times. Cells were immunostained with anti-IdU/BrdU antibody and the percentages of IdU-positive cells were determined. Values represent the mean±s.d. of three independent experiments. **P*<0.05, ***P*<0.01 versus Vehicle. (D) OUMS/Tet-on shHSF1 cells treated with vehicle or DOX for the indicated times were subjected to the SA-β-gal assay. SA-β-gal-positive cells were counted and the percentages of positive cells were calculated. Values represent the mean±s.d. of three independent experiments. **P*<0.05, ***P*<0.01 versus Vehicle. (E) Similarly, OUMS/Tet-on shHSF1 cells were treated with DOX and stained with DAPI. Then, SAHF-positive cells were counted and the percentages of positive cells were calculated. Values represent the mean±s.d. of three independent experiments. **P*<0.05 versus Vehicle. (F) OUMS/Tet-on shHSF1 cells were treated with vehicle or DOX for 12 days. Cells were fixed with 70% ethanol, stained with propidium iodide and subjected to flow cytometry. FSC-SSC plots of each sample are shown, and the numbers indicate the percentages of F2 (left panels). DNA-content histograms of cells from F1 and F2 are shown (middle panels), and the percentages of cells in G1-, S- and G2-phases were determined using FlowJo software (right graph). Values represent the mean±s.d. of three independent experiments. (G) Total RNA was prepared from OUMS/Tet-on shHSF1 cells treated with DOX for the indicated times and qPCR was performed to determine the mRNA levels of the indicated genes. Values represent the mean±s.d. of triplicate wells. Similar results were obtained from two independent experiments. (H) OUMS/Tet-on shHSF1 cells were lentivirally transduced with shHSF1-resistant WT HSF1 (WT). Three days after infection, cells were selected in the presence of 40 µg/ml blasticidin S for 3 days. Then, cells were treated with vehicle or DOX for 7 days and whole-cell lysates were prepared and immunoblotted (left panels). OUMS/Tet-on shHSF1 cells transduced with empty vector were used as controls (Vector). In parallel, cells treated with vehicle or DOX for 9 days were subjected to the SA-β-gal assay (right graph). Values represent the mean±s.d. of three independent experiments. ***P*<0.01 versus Vector/DOX.

into OUMS/Tet-on shHSF1 cells. While E6 expression did not affect the DOX-induced depletion of HSF1, it markedly suppressed the consequent increases in p53 and p21, and the induction of SA-β-gal-positive cells (Fig. 3B). Consistently, shRNA-mediated depletion of p53 suppressed the induction of p21 and SA-β-gal-positive cells, and partially restored the DOX-induced suppression of DNA synthesis (Fig. 3C and Fig. S3E). In addition, shRNA-mediated depletion of p21 suppressed the number of SA-β-gal-positive cells and partially restored the DOX-induced suppression of DNA synthesis (Fig. 3C and Fig. S3E). Collectively, these results indicate that HDIS is mediated by activation of the p53-p21 pathway.

Kim et al. have previously reported that activation of the p38 MAPK pathway is involved in HDIS within human diploid cells (Kim et al., 2012). To monitor the activation of this pathway in our experimental system, we measured the phosphorylation levels of p38 MAPK and its substrate HSPB1 (Hsp27). Our results indicate that HSF1 depletion had little effect on the phosphorylation levels of p38 MAPK and HSPB1 (Fig. S3F). Furthermore, HDIS was not suppressed by treatment with the p38 MAPK inhibitor SB203580 (Fig. S3G). Together, these results indicate that the p38 MAPK pathway is not involved in HDIS in our system. This discrepancy might be explained by differences in cell type or experimental conditions between the previous study and ours.

HSF1 depletion suppresses the MDM2-dependent degradation of p53

The increased p53 protein levels after HSF1 depletion were not associated with increased levels of its mRNA in OUMS/Tet-on shHSF1 cells (Fig. S3B). Thus, we reasoned that the increased steady-state levels of p53 may be due to its increased protein stability (Bieging et al., 2014; Kruse and Gu, 2009; Manfredi, 2010). To test this notion, we performed cycloheximide (CHX) chase experiments. The results showed that the half-life of p53 was prolonged from ∼40 min in the control cells (vehicle-treated) to ∼3 h or longer in the HSF1-depleted cells (DOX-treated), indicating that HSF1 depletion increased the stability of p53 (Fig. 4A,B). Next, we hypothesized that decreased activity of MDM2, the major E3 ligase of p53 (Manfredi, 2010; Wade et al., 2013), may mediate the p53 stabilization in HSF1-depleted cells. To test this hypothesis, we examined the effect of Nutlin-3, a specific inhibitor of MDM2, on the stability of p53. CHX chase analysis revealed that Nutlin-3 drastically increased the stability of p53 in control OUMS/Tet-on shHSF1 cells, indicating that MDM2 is responsible for most (> 80%) of the p53 degradation in these cells. Of note, DOX treatment for 7 days suppressed p53 degradation to a large extent (60–70%) (Fig. 4A), suggesting that this suppression is, at least in part, mediated by decreased MDM2 activity. Furthermore, Nutlin-3 had only a minimal effect on p53 stability in DOX-treated cells. Collectively, these results suggest that the p53 stabilization in the HSF1-depleted cells is largely attributable to MDM2 inhibition (Fig. 4A). Similar but less stabilization of p53 was detected in cells treated with DOX for 4 days (Fig. 4B), suggesting that the inhibition of MDM2 progressively increased at 4–7 days after DOX treatment in OUMS/Tet-on shHSF1 cells. Finally, we examined the effects of HSF1 depletion on the polyubiquitylation of p53. Consistent with the above notion, Nutlin-3 and DOX treatment decreased the levels of K48-linked polyubiquitylated p53 to similar extents (Fig. 4C). Overall, our results indicate that HSF1 depletion increases p53 levels by inhibiting its degradation through the MDM2-proteasome pathway.

HSF1 transcriptional activity is required for the suppression of cellular senescence

The observations that HSF1 regulates cellular senescence in a manner independent of HSP expression prompted us to test whether the transcriptional activity of HSF1 is required for its regulatory function in senescence because some studies reported that HSF1 regulated cell growth independent of transcriptional regulation (Lee et al., 2008; Su et al., 2016). To address this issue, we took advantage of OUMS/Tet-on shHSF1 cells in which shHSF1 targets the sequence in the 3′-UTR of *HSF1* mRNA as described above, thus allowing the ectopic expression of cDNAs encoding HSF1 proteins. We used four known mutants with K80Q or R71G amino acid residue substitution in the DNA-binding domain, or deletion of the trimerization domain (Δ156–226) or activation domain (Δ454–529) (Fig. 5A). These mutants lose transcriptional activity for *HSPA1A* (Inouye et al., 2003; Verma et al., 2014; Wang et al., 2002; Westerheide et al., 2009).

Lentiviral introduction of WT or mutant *HSF1* cDNAs into OUMS/Tet-on shHSF1 cells allowed expression of the encoded proteins in >90% of the cells (data not shown). Overexpression of WT-HSF1, but not of mutant proteins, increased *HSPA1A* mRNA in control and DOX-treated cells (Fig. 5B). Although treatment with the HSP90 inhibitor 17-allylamino-17-demethoxy-geldanamycin (17-AAG) further increased *HSPA1A* mRNA levels in WT-HSF1-expressing cells, such effects were not observed in mutant HSF1-expressing cells (Fig. 5B), confirming that these mutants lost their transcriptional activity. Importantly, expression of these mutant HSF1 proteins failed – unlike WT-HSF1 – to suppress the DOX-induced increase in SA-β-gal-

Journal of Cell Science (2018) 131, jcs210724. doi:10.1242/jcs.210724

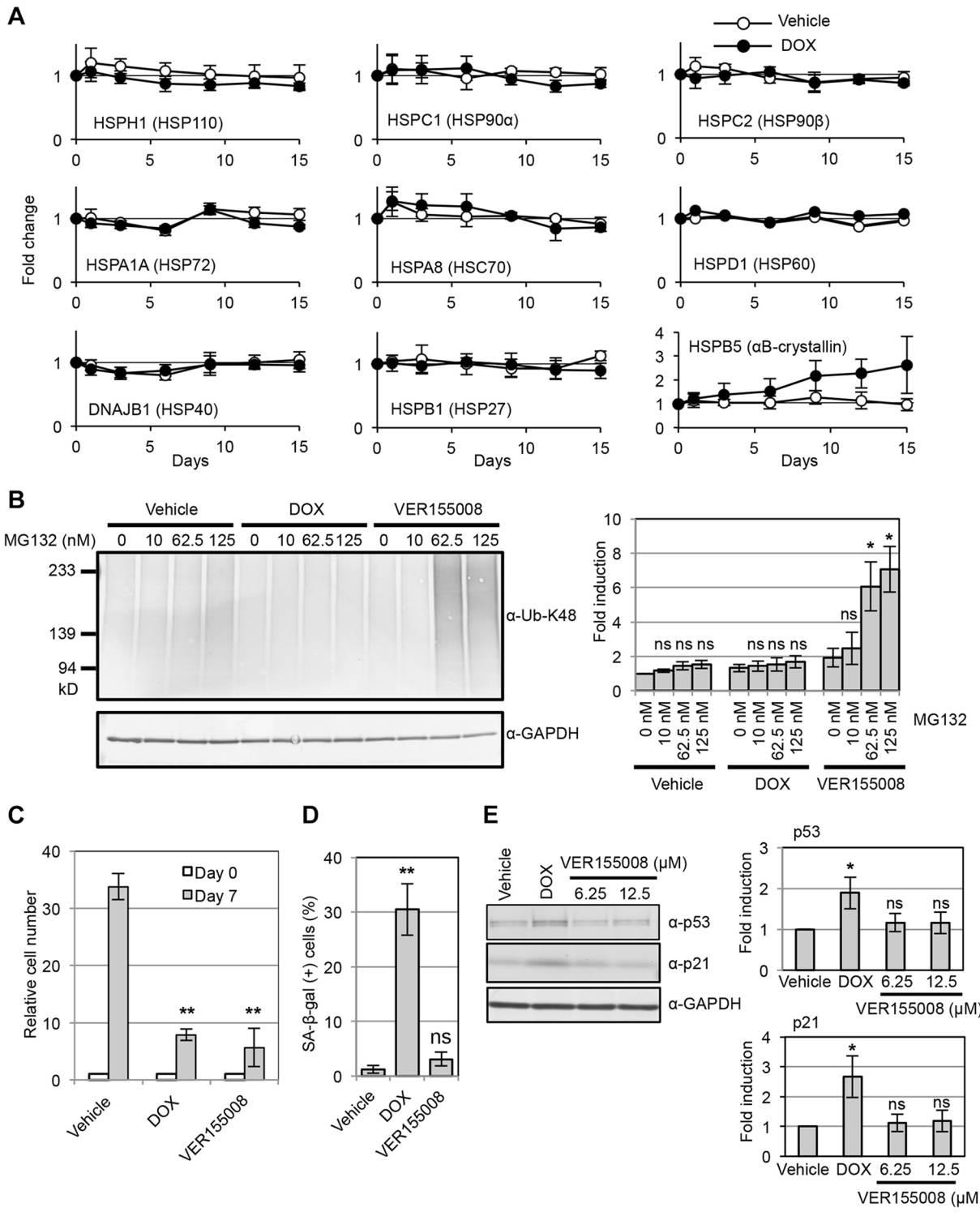

Fig. 2. HDIS is not associated with reduced expression of HSPs or increased proteotoxic stress. (A) OUMS/Tet-on shHSF1 cells were treated with vehicle or DOX for the indicated times and whole-cell lysates were immunoblotted with the indicated antibodies (refer to Fig. S2A). Signals of HSPs and GAPDH were densitometrically quantified as described in the Materials and Methods. HSPs signals were normalized against GAPDH signals and fold changes of HSPs levels were calculated with reference to Day 0. The horizontal line at 1 indicates the basal line. Values represent the mean±s.d. of three independent experiments. (B) OUMS/Tet-on shHSF1 cells were treated with vehicle, DOX or 12.5 μM VER155008 for 7 days, and with the indicated concentrations of MG132 for the last 24 h. Whole-cell lysates were prepared and immunoblotted with the indicated antibodies (left panels). K48-linked ubiquitin (Ub-K48) signals were quantified and normalized against GAPDH signals (right graph). Values represent the mean±s.d. of three independent experiments. *P<0.05 vs 0 nM MG132; ns, not significant. (C,D) OUMS/Tet-on shHSF1 cells treated with vehicle, DOX or VER155008 for 7 days. Relative cell numbers (C) and the percentage of SA-β-gal-positive cells (D) were determined. Values represent the mean±s.d. of three independent experiments. **P<0.01 versus Vehicle; ns, not significant. (E) Whole-cell lysates were prepared from OUMS/Tet-on shHSF1 cells treated with vehicle, DOX or VER155008 (6.25 and 12.5 μM) for 7 days and immunoblotted (left panels). p53 and p21 signals were quantified and normalized against GAPDH signals (right graphs). Values represent the mean±s.d. of three independent experiments. *P<0.05 versus Vehicle; ns, not significant.

Journal of Cell Science (2018) 131, jcs210724. doi:10.1242/jcs.210724

positive cells (Fig. 5C). Furthermore, WT-HSF1, but not the mutant proteins, suppressed the DOX-induced increase in p53 and p21 (Fig. 5D). Collectively, these results indicate that the transcriptional activity of HSF1 plays a central role in the regulation of HDIS.

DHRS2, an MDM2-binding protein, is upregulated in HSF1-depleted cells

Overall, our observations suggest that a non-HSP target gene(s) of HSF1 regulate the MDM2-mediated p53 stability and cellular senescence. To search for such target gene(s), we performed microarray gene expression analysis comparing control (day 0) and OUMS/Tet-on shHSF1 cells treated with DOX for 1, 3 or 7 days. The gene expression data of 144 MDM2 regulators reported in the literature are shown as a heat map (Fig. S4). We found that mRNA levels of *DHRS2*, a member of the NAD/NAD(P)-dependent oxidoreductase superfamily and a putative MDM2 inhibitor (Deisenroth et al., 2010), increased the most, at days 3 and 7 after DOX treatment (Fig. S4). Interestingly, the *DHRS2* gene had been reported to be a potential target of HSF1 (Hayashida et al., 2010; Hensen et al., 2013). These findings led us to pursue the role of DHRS2 in HDIS. The pronounced induction of DHRS2 was confirmed by quantitative polymerase chain reaction (qPCR) analysis (∼15-fold increase in mRNA levels at days 3 and 7; Fig. 6A) and immunoblot analysis (Fig. 6B). Furthermore, the time course of this DHRS2 increase was consistent with those of p53 upregulation (Fig. 3A) and increased stability of p53 (Fig. 4A,B). The increase in *DHRS2* mRNA was also detected in HSF1-depleted HDFs, MRC-5 and TIG-3 (Fig. 6C). Together, these results suggest that transcription of the *DHRS2* gene is negatively regulated by HSF1. Further supporting this notion, the DOX-induced increase in *DHRS2* mRNA levels was suppressed by the expression of WT-HSF1 but not by the mutant HSF1 proteins (K80Q, R71G, Δ156–226 and Δ454–529) lacking transcriptional activity (Fig. 6D).

The *DHRS2* gene had been reported to be a potential target of HSF1 (Hayashida et al., 2010; Hensen et al., 2013). Therefore, we investigated whether HSF1 directly regulates transcription of the *DHRS2* gene. Two main RNAs are transcribed from the *DHRS2* gene (XM_005267249.1 and NM_005794.3 are shown as representative samples, Fig. S5A). We found 12 and 6 potential heat-shock-responsive elements (HREs) consisting of more than three inverted nGAAn repeats (Fujimoto et al., 2012; Guertin and Lis, 2010; Trinklein et al., 2004), upstream (< ∼6000 bp) of these transcription initiation sites, (Fig. S5B,C). To determine whether HSF1 binds to these potential HREs, chromatin immunoprecipitation (ChIP) and qPCR were performed. As reported previously (Fujimoto et al., 2012), specific binding of HSF1 to the HRE of *HSPA1A* was detected in vehicle-treated OUMS/Tet-on shHSF1 cells under non-stress conditions (Fig. S5D). This binding was greatly diminished in the DOX-treated OUMS/Tet-on shHSF1 cells, confirming the shRNA-mediated depletion of HSF1 (Fig. S5D). Under the same conditions, HSF1 binding to the potential HREs of *DHRS2* was negligible (Fig. S5D). Furthermore, in OUMS/Tet-on shHSF1 cells overexpressing WT-HSF1 (data not shown), HSF1-binding to the HRE of *HSPA1A* increased ∼5-fold (Fig. S5E), but HSF1 binding to the potential HREs of *DHRS2* was still undetectable (Fig. S5E). These results suggest that the *DHRS2* gene is not a direct target of HSF1.

DHRS2 partly mediates HSF1 depletion-induced p53 stabilization and cellular senescence in HDFs

Deisenroth et al. have proposed that DHRS2 regulates p53 stability, based on the observations that DHRS2 binds MDM2 and increases the steady-state levels of p53 (Deisenroth et al., 2010). To verify this notion, we used tumor cells, including U2OS and MCF7 cells, with high endogenous levels of *DHRS2* mRNA and WT *p53* alleles (Fig. S6A). Consistent with the previous results, an interaction between MDM2 and DHRS2 was detected in U2OS cells (Fig. S6B) (Deisenroth et al., 2010). In addition, the introduction of two different shRNAs targeting DHRS2 (shDHRS2s #1 and #2) reduced the steady-state levels of p53 and p21 in these cells (Fig. S6C). Notably, MDM2 levels were unchanged by DHRS2 depletion. Similar results were obtained in DHRS2-depleted MCF7 cells (Fig. 7A). To assess the regulatory role of DHRS2 in the stability of p53, we performed CHX chase experiments. As expected, the shRNA-mediated depletion of DHRS2 significantly reduced the stability of p53 in MCF7 cells (Fig. 7A). Together, these results support the notion that DHRS2 is a negative regulator of MDM2 and that its expression levels affect the stability of p53.

We next examined the regulatory role of DHRS2 on the MDM2-p53-p21 pathway in OUMS/Tet-on shHSF1 cells. For this purpose, we introduced shDHRS2s #1 and #2 into these cells. These shDHRS2s reduced DHRS2 protein levels, and significantly suppressed DOX-induced DHRS2 expression and the increase in p53 and p21 levels (Fig. 7B and Fig. S6D). We reasoned that these effects may be attributed to decreased p53 stability resulting from DHRS2 depletion. To test this notion, we performed CHX chase analysis. We found that shDHRS2 moderately, but significantly, reduced the DOX-induced p53 stabilization (Fig. 7C). Consistently, the DOX-induced decrease in p53 polyubiquitylation was suppressed in shDHRS2-expressing cells (Fig. 7D, lanes 5 and 6) compared with the control cells (Fig. 7D, lane 4).

Furthermore, we studied the role of DHRS2 in HDIS. For this purpose, we introduced shDHRS2 #1 or #2 into OUMS/Tet-on shHSF1 cells and evaluated their effects on HDIS using different assays. Introduction of these shDHRS2s partially recovered the DOX-induced growth suppression (Fig. 8A) and, moderately but significantly, suppressed the DOX-induced increase in the number of SA-β-gal-positive cells (Fig. 8B). Consistently, the DOX-induced increase in the percentages of enlarged senescent cells was significantly suppressed in cells expressing shDHRS2s (Fig. 8C). Together, these results indicate that HDIS is partly mediated by the increased expression of DHRS2.

DISCUSSION

Loss of HSF1 suppresses tumorigenesis and promotes aging (Anckar and Sistonen, 2011; Gomez-Pastor et al., 2017; Labbadia and Morimoto, 2015). Given the crucial roles of cellular senescence in tumorigenesis and aging-related phenotypes (Campisi, 2013; He and Sharpless, 2017; Muñoz-Espín and Serrano, 2014), understanding the molecular mechanisms of HDIS is expected to provide an important insight into these functions. There are two different, though not mutually exclusive, views on the mechanisms by which HSF1 promotes cell growth and survival. One widely accepted view is that these functions of HSF1 are mediated by HSP-dependent proteostasis. The other suggests that the HSF1-regulated expression of various non-HSP genes is involved in fundamental cellular functions (Hahn et al., 2004; Mendillo et al., 2012; Takii et al., 2015). In agreement with the former view, a previous paper reported that HDIS is associated with decreased expression of HSPs and activation of the p38 MAPK-SASP pathway but not p53 activation in HDFs (Kim et al., 2012). By contrast, our present study provides evidence that HDIS is not associated with either the reduced expression of HSPs and impaired proteostasis or p38

Journal of Cell Science (2018) 131, jcs210724. doi:10.1242/jcs.210724

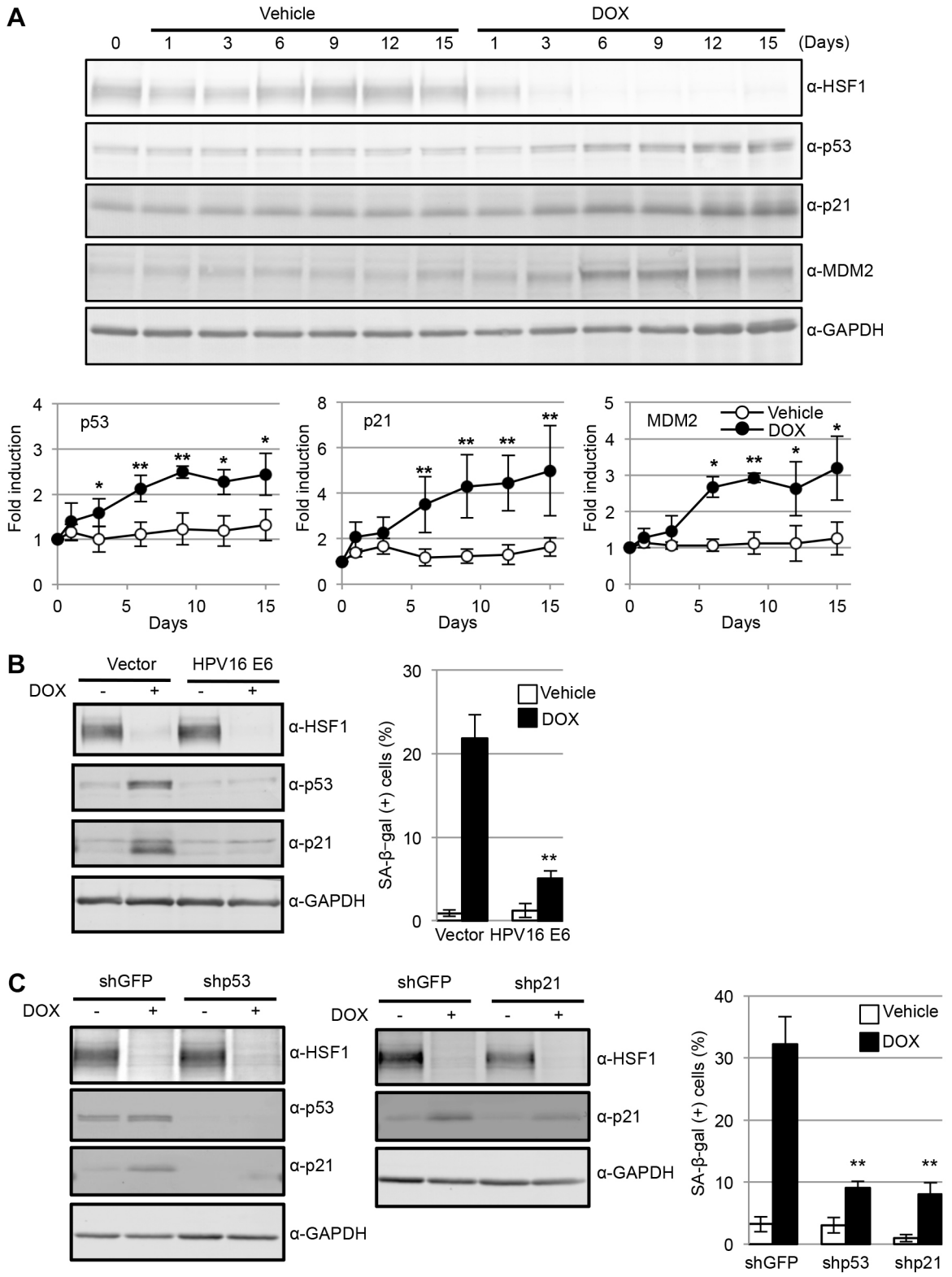

Fig. 3. HDIS is mediated by activation of the p53-p21 pathway. (A) OUMS/Tet-on shHSF1 cells were incubated with vehicle or DOX for the indicated times. Whole-cell lysates were prepared and immunoblotted with the indicated antibodies (top panels). p53, p21 and MDM2 signals were quantified and normalized against GAPDH signals (graphs). Values represent the mean±s.d. of three independent experiments. **P*<0.05, ***P*<0.01 versus Vehicle. (B) OUMS/Tet-on shHSF1 cells stably expressing HPV16 E6 were treated with vehicle (–) or DOX (+) for 13 days. Whole-cell lysates were prepared and immunoblotted (left panels), and cells were subjected to the SA-β-gal assay (right graph). Values represent the mean±s.d. of three independent experiments. ***P*<0.01 versus Vector/DOX. (C) OUMS/Tet-on shHSF1 cells were lentivirally transduced with shGFP, shp53, or shp21. Three days after infection, cells were selected for 3 days in the presence of 40 µg/ml blasticidin S. Then, the cells were incubated with vehicle (–) or DOX (+) for 8 days. Whole-cell lysates were prepared and immunoblotted with the indicated antibodies (left panels), and cells were subjected to the SA-β-gal assay (right graph). Values represent the mean±s.d. of three independent experiments. ***P*<0.01 versus shGFP/DOX.

Journal of Cell Science (2018) 131, jcs210724. doi:10.1242/jcs.210724

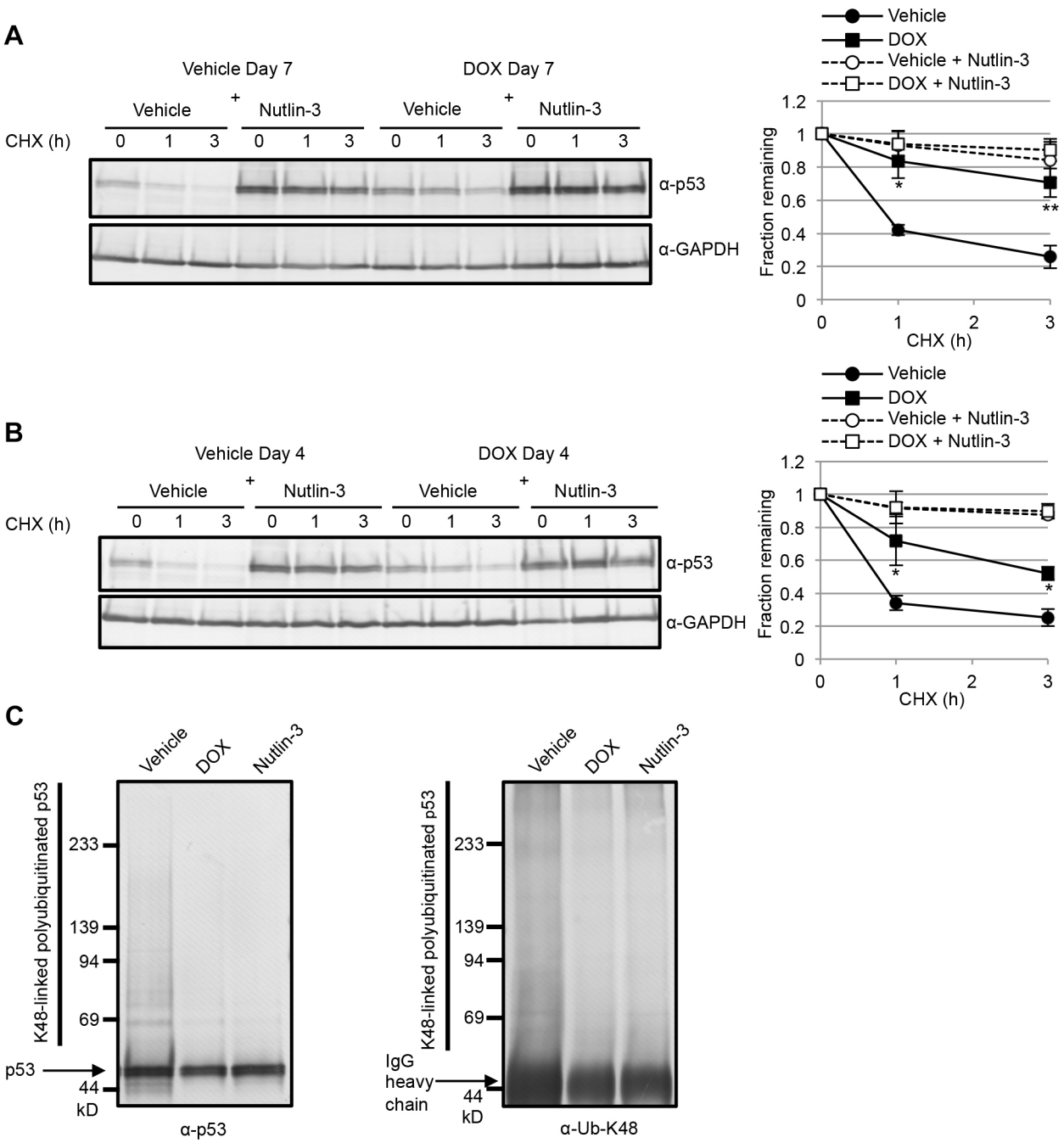

Fig. 4. HSF1 depletion suppresses the MDM2-dependent degradation of p53. (A,B) OUMS/Tet-on shHSF1 cells were treated with vehicle or DOX for 7 days (A) or 4 days (B). Cells were incubated with vehicle or 10 µM Nutlin-3 for the last 24 h and then 100 µg/ml CHX was added to the culture medium. After 0, 1 and 3 h, whole-cell lysates were prepared and immunoblotted (left panels). The p53 signals were quantified and normalized against GAPDH signals (right graphs). Values represent the mean±s.d. of three independent experiments. *P<0.05 versus Vehicle; **P<0.01 versus Vehicle. (C) OUMS/Tet-on shHSF1 cells treated with vehicle or DOX for 7 days, or Nutlin-3 for 2 h were lysed with RIPA buffer. p53 was immunoprecipitated from the lysates with rabbit anti-p53 antibody and the immunoprecipitates were immunoblotted with mouse anti-p53 antibody (left) or anti-K48-linked ubiquitin (Ub-K48) antibody (right). Similar results were obtained from two independent experiments.

MAPK activation but rather depends on activation of the p53-p21 pathway in HDFs. To illustrate the difference between the two studies, schematic models are shown in Fig. S7. Importantly, we found that DHRS2, a protein recently reported to bind and inhibit MDM2 (Deisenroth et al., 2010), is involved in p53-p21 activation in HDIS. To our knowledge, this is the first report indicating a molecular pathway in which HSF1-mediated gene expression leads to p53-p21 activation and cellular senescence.

To study the molecular mechanisms of HDIS, we generated an immortalized HDF clone in which the drug-induced expression of shHSF1 reproducibly induced cellular senescence that was suppressed by the ectopic expression of WT-HSF1. During the course of HDIS of these cells, the expression levels of main HSPs exhibited little change. In addition, the single-cell analysis of shHSF1-transduced cells revealed no significant difference in HSPA1A levels between senescent and non-senescent populations.

Journal of Cell Science (2018) 131, jcs210724. doi:10.1242/jcs.210724

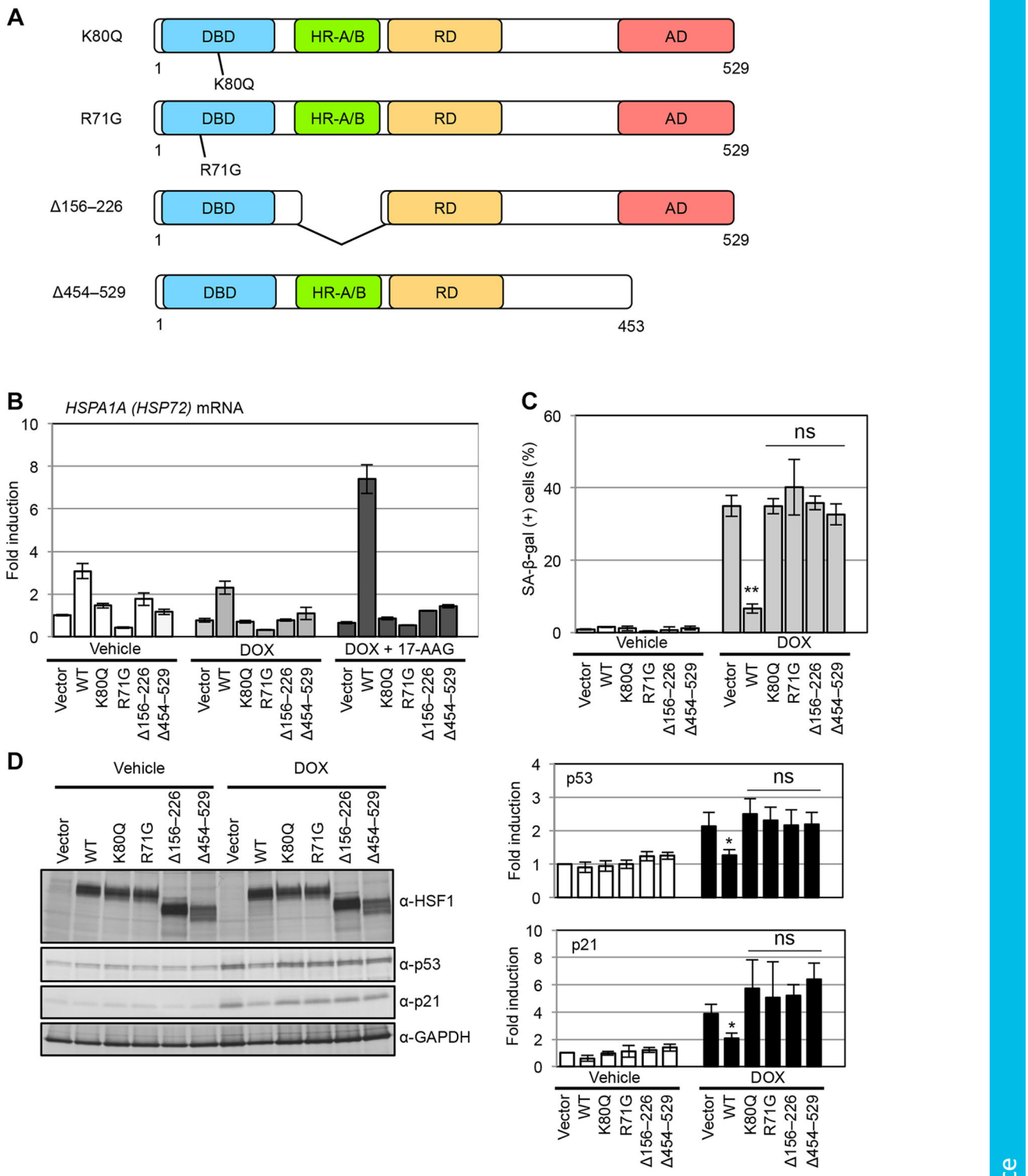

Fig. 5. Transcriptional activity of HSF1 is required for the suppression of cellular senescence. (A) Schematic illustration of HSF1 mutants. The numbers indicate amino acid positions in HSF1. The DNA-binding domain (DBD), two hydrophobic repeats (HR-A/B), regulatory domain (RD) and transactivation domain (AD) of HSF1 are shown. Amino acid substitution mutants (K80Q, R71G) and deletion mutants (Δ156–226, Δ454–529) are shown. (B) OUMS/Tet-on shHSF1 cells were lentivirally transduced with an empty vector or vectors encoding either shHSF1-resistant WT or mutant HSF1 (K80Q, R71G, Δ156–226 or Δ454–529) proteins. Three days after infection, cells were selected in the presence of 40 µg/ml blasticidin S for 3 days. Then, the cells were incubated with vehicle or DOX for 7 days. In parallel, DOX-treated cells were treated with 500 nM 17-AAG for the last 8 h of incubation (DOX+17-AAG). Total RNA was prepared and *HSPA1A* mRNA levels were measured by qPCR. Values represent the mean±s.d. of triplicate wells. Similar results were obtained from two independent experiments. (C) OUMS/Tet-on shHSF1 cells stably expressing WT or mutants HSF1 described in (B) were treated with vehicle or DOX for 9 days and subjected to the SA-β-gal assay. Values represent the mean±s.d. of three independent experiments. ***P*<0.01 versus Vector/DOX; ns, not significant. (D) Whole-cell lysates from cells treated with vehicle or DOX for 7 days were immunoblotted with the indicated antibodies (left panels). A rat monoclonal anti-HSF1 antibody with an epitope localized in the central region was used in this experiment. The p53 and p21 signals were quantified and normalized against GAPDH signals (right graphs). Values represent the mean±s.d. of three independent experiments. **P*<0.05 versus Vector/DOX; ns, not significant.

Journal of Cell Science (2018) 131, jcs210724. doi:10.1242/jcs.210724

Furthermore, HSF1 depletion did not affect proteostasis as estimated by total polyubiquitylated protein levels, while treatment of these cells with an inhibitor of HSP70 family proteins impaired proteostasis and suppressed cell growth but did not induce senescence. Collectively, these data indicate that HDIS of non-transformed HDFs is not associated with HSP-mediated proteostasis.

The p53-p21 pathway plays a central role in cellular senescence induced by various stressors (Campisi, 2013; He and Sharpless, 2017; Muñoz-Espín and Serrano, 2014). We demonstrated that activation of this pathway by reduced MDM2 activity is required for HDIS. Moreover, we showed that HDIS or HSF1 depletion-induced p53 upregulation is suppressed by the ectopic expression of WT-HSF1 protein but not by its mutant proteins lacking transcriptional activity. These two lines of evidence prompted us to search for an MDM2 regulator(s) in HSF1-regulated genes. We, therefore, performed microarray experiments to analyze alteration in the gene expression profile during the DOX-induced HDIS of OUMS/Tet-on shHSF1 cells. We found that the mRNA levels of *DHRS2* increased to the largest extent among a number of MDM2 regulators, with kinetics similar to that of p53 induction. In addition, previous studies have reported that *DHRS2* is a potential target of HSF1 (Hayashida et al., 2010; Hensen et al., 2013). Thus, we studied whether DHRS2 contributes to HDIS. We first confirmed that DHRS2 binds to MDM2 and regulates p53 stability in human tumor cells. Furthermore, we showed that the knockdown of DHRS2 significantly suppressed the stabilization and upregulation of p53 and HDIS in DOX-treated OUMS/Tet-on shHSF1 cells. Thus, we conclude that DHRS2 plays a significant role in the molecular pathway of the HSF1 depletion-induced p53-p21 activation and senescence. However, our data indicate that HSF1 does not directly bind to the promoter region of the *DHRS2* gene, which raises the question of what the direct target of HSF1 is in this pathway.

The effects of DHRS2 knockdown on p53 levels were modest, especially until the later phase of DOX-induced HDIS. One possible reason is that the efficiency of shDHRS2-mediated knockdown is relatively mild in OUMS/Tet-on shHSF1 cells. This notion is supported by the observation that the shDHRS2-mediated depletion of its protein product and p53 levels were more pronounced in U2OS and MCF7 cells. More importantly, it is likely that MDM2 regulators other than DHRS2 are involved in HSF1 depletion-induced p53 stabilization. Given that multiple positive and negative regulatory proteins of MDM2 can alter mRNA expression during HDIS, these proteins might contribute to p53 stabilization in HDIS. In addition, there is an increasing number of modulators that affect the MDM2-p53 pathway in a cellular- and context-dependent manner (Fåhraeus and Olivares-Illana, 2014; Li and Kurokawa, 2015). For instance, microRNAs, an emerging group of such regulators, might mediate HSF1 (Hoffman et al., 2014). To find a regulator(s) of the MDM2-p53 pathway during HDIS is an important aim in future studies.

Although Hsf1-null mice exhibit placental defects and prenatal lethality in a strain-dependent manner, remaining mice survive to adulthood, which is unlikely to reflect HDIS. This apparent discrepancy can be partly explained by genetic compensation in these mice through other heat shock factors and/or the adaptive alteration of Hsf1 signaling/transcriptional networks, rather than to a difference in species. Indeed, there have been many reports of similar cases of knockout organisms that exhibited unexpectedly mild or negligible phenotypes from knockdown effects (El-Brolosy and Stainier, 2017). Importantly, in some of these organisms, appropriate stresses uncover hidden phenotypes. In this context, it is tempting to speculate that some phenotypes of Hsf1-null mice can be explained by the potentiation of stress-induced p53 activation and senescence (Campisi, 2013; He and Sharpless, 2017; Muñoz-Espín and Serrano, 2014). For instance, tumor suppression in Hsf1-null mice can be

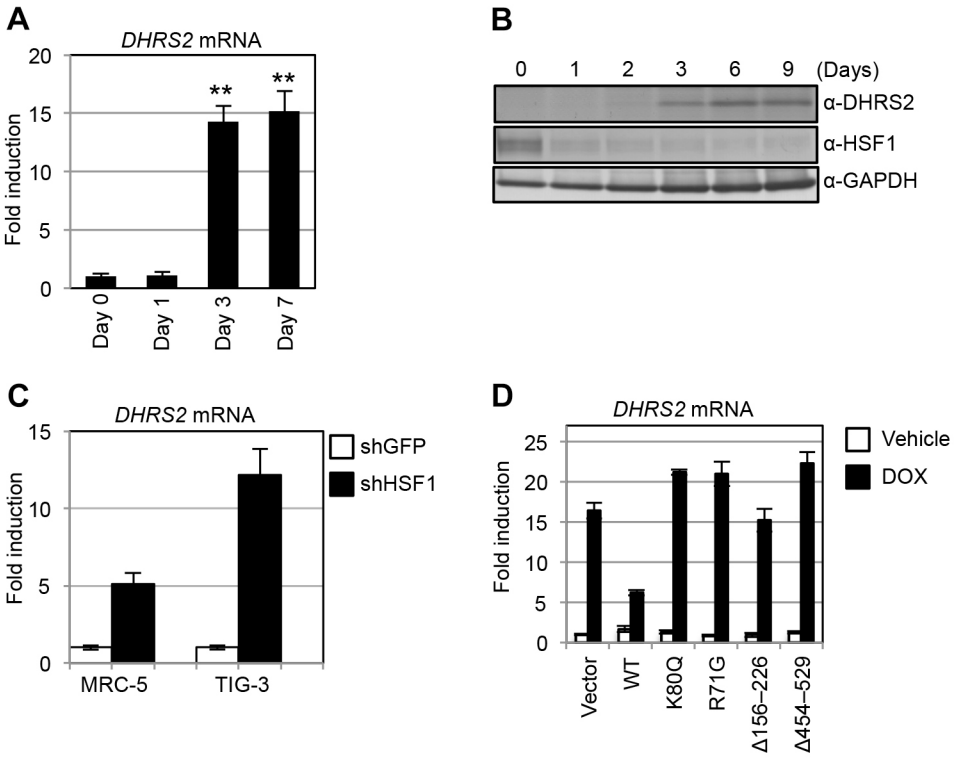

Fig. 6. DHRS2, a negative regulator of MDM2, is upregulated in HSF1-depleted cells. (A) Total RNA was prepared from OUMS/Tet-on shHSF1 cells treated with DOX for the indicated times. qPCR analysis was performed to measure the mRNA levels of *DHRS2*. Values represent the mean±s.d. of three independent experiments. ***P*<0.01 versus Day 0. (B) Whole-cell lysates were prepared from OUMS/Tet-on shHSF1 cells treated with DOX for the indicated times and immunoblotted with the indicated antibodies. Similar results were obtained from two independent experiments. (C) MRC-5 and TIG-3 cells were infected with lentivirus and selected in the presence of 1 µg/ml puromycin for 3 days. Total RNA was prepared and *DHRS2* mRNA levels were measured by qPCR. Values represent the mean±s.d. of triplicate wells. (D) OUMS/Tet-on shHSF1 cells stably expressing either WT or mutant HSF1 proteins described in Fig. 5 were treated with vehicle or DOX for 7 days. Total RNA was prepared and *DHRS2* mRNA levels were measured by qPCR. Values represent the mean±s.d. of triplicate wells. Similar results were obtained from two independent experiments.

Journal of Cell Science (2018) 131, jcs210724. doi:10.1242/jcs.210724

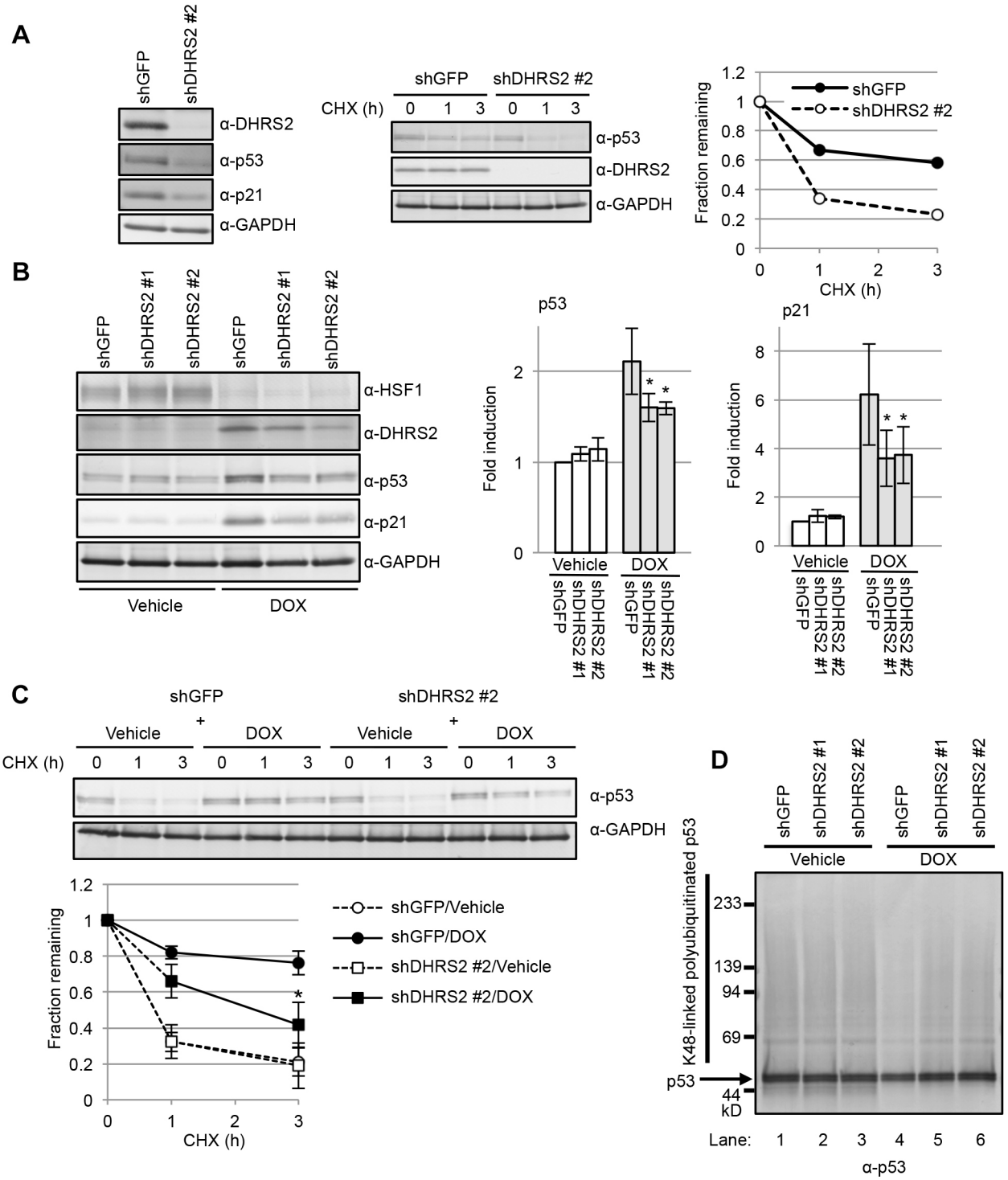

Fig. 7. DHRS2 partly mediates HSF1 depletion-induced p53 stabilization. (A) MCF7 cells were lentivirally transduced with shGFP or shDHRS2 #2. Three days after infection, cells were selected in the presence of 40 µg/ml blasticidin S for 3 days. Whole-cell lysates were prepared and immunoblotted with the indicated antibodies (left). Furthermore, cells were incubated with 100 µg/ml CHX for the indicated times and whole-cell lysates were immunoblotted (middle). p53 signals were quantified and normalized against GAPDH signals (right). Similar results were obtained from two independent experiments. (B) OUMS/Tet-on shHSF1 cells were lentivirally transduced with shGFP, shDHRS2 #1, or shDHRS2 #2. Three days after infection, cells were selected in the presence of 40 µg/ml blasticidin S for 3 days. Then, cells were treated with vehicle or DOX for 9 days. Whole-cell lysates were prepared and immunoblotted with the indicated antibodies (left). p53 and p21 signals were quantified and normalized against GAPDH signals (middle and right). Values represent the mean±s.d. of three independent experiments. *P<0.05 versus shGFP/DOX. (C) OUMS/Tet-on shHSF1 cells expressing shGFP or shDHRS2 #2 were treated with vehicle or DOX for 7 days. Then, cells were treated with CHX for the indicated times as described in Fig. 4A,B. Whole-cell lysates were immunoblotted with the indicated antibodies (top); p53 signals were quantified and normalized against GAPDH signals (bottom). Values represent the mean±s.d. of three independent experiments. *P<0.05 versus shGFP/DOX. (D) OUMS/Tet-on shHSF1 cells expressing shGFP, shDHRS2 #1 or shDHRS2 #2 were treated with vehicle or DOX for 7 days and lysed with RIPA buffer. p53 was immunoprecipitated from the lysates using rabbit anti-p53 antibody and immunoblotted with mouse anti-p53 antibody as described in Fig. 4C.

Journal of Cell Science (2018) 131, jcs210724. doi:10.1242/jcs.210724

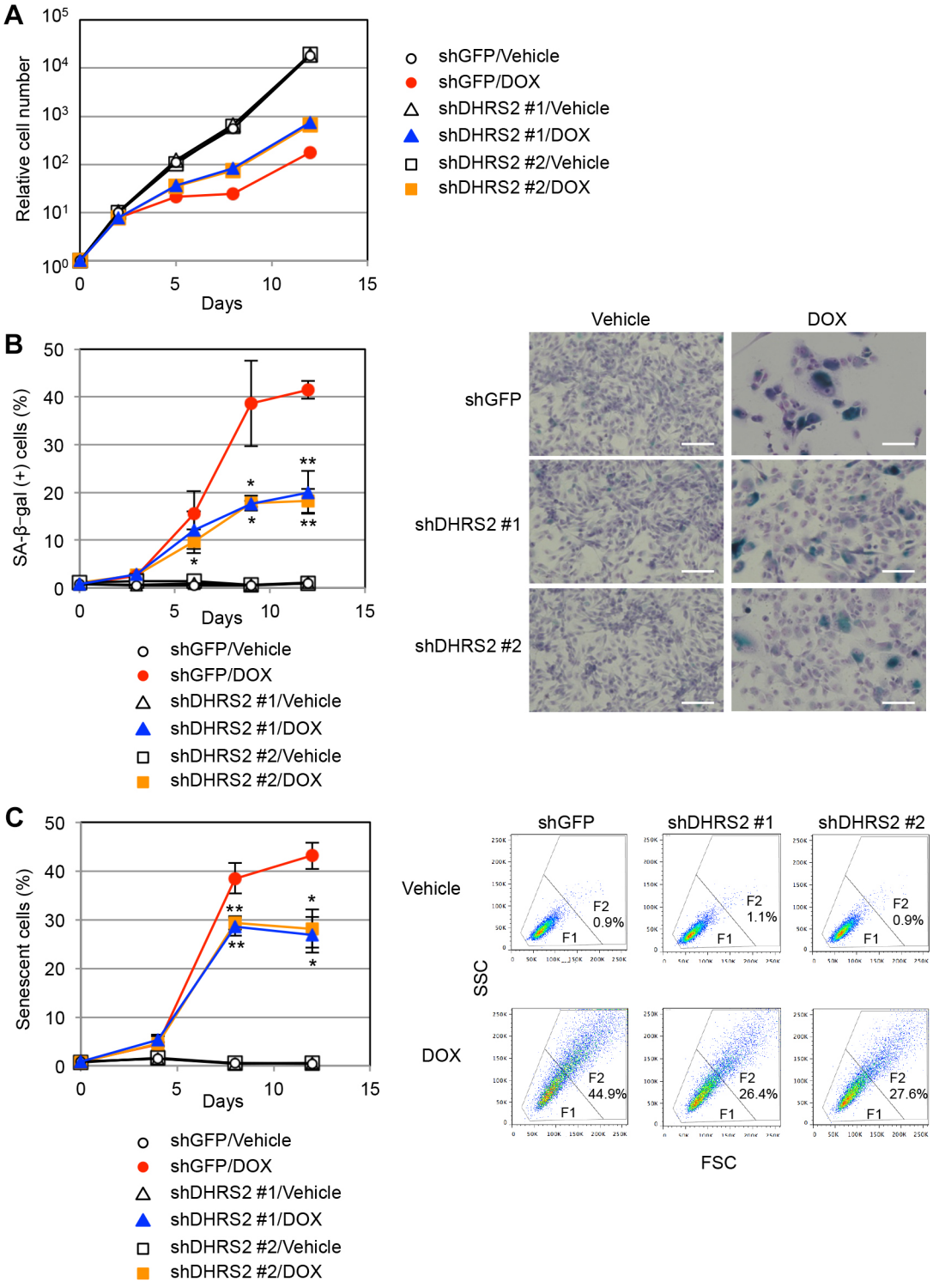

Fig. 8. DHRS2 partly mediates HDIS in HDFs. OUMS/Tet-on shHSF1 cells expressing shGFP, shDHRS2 #1 or shDHRS2 #2 described in Fig. 7B were treated with vehicle or DOX. (A) Relative cell numbers were determined at the indicated times. Similar results were obtained from three independent experiments. (B) Cells were subjected to the SA-β-gal assay and the percentage of positive cells was determined at the indicated times (left). Values represent the mean±s.d. of three independent experiments. **P*<0.05, ***P*<0.01 versus shGFP/DOX. Representative images of day 8 are shown (right). Scale bars: 100 µm. (C) Cells were subjected to flow cytometry analysis at the indicated times as described in Fig. 1F and the percentages of senescent cells (F2) were determined (left). Values represent the mean±s.d. of three independent experiments. **P*<0.05, ***P*<0.01 versus shGFP/DOX. Representative results of day 9 are shown (right).

partly explained by the synergistic induction of senescence in the presence of oncogenic stress. In favor of this notion, HDIS is negligible in the immortalized human mammary epithelial cell line MCF10A and the hTERT-immortalized human retinal pigment epithelial cell line (RPE-1), but is synergistically induced after oncogene activation (Meng et al., 2010; our unpublished

observations). We postulate that careful analyses of the phenotypes in Hsf1-null mice experiencing senescence-inducing stresses might provide insights into the *in vivo* functions of HDIS.

Our present findings raise important clinical and biological issues. First, our observations highlight the importance to study the effects of HSF1 inhibitors on normal cells. Although increasing numbers of studies regard them as promising agents for cancer therapy, most of them suggest that the effect of HSF1 inhibition on the growth of non-transformed cells is negligible (Dai et al., 2007; Meng et al., 2010; Tang et al., 2015). This discrepancy with our results can be explained by differences in cell type or experimental condition used, because most of the preceding studies used epithelial cells, such as MCF10A cells, and examined short-time effects. To support this notion, we observed that HSF1 depletion induced minimal cellular senescence in RPE-1 cells, another immortalized non-transformed epithelial cell line (our unpublished data). Therefore, careful preclinical studies with attention to HDIS in various types of non-transformed cell are required. Moreover, the *in vivo* roles of HDIS in the development of tumors and aging-related pathologies are important topics for future studies. Given the increasing evidence that protein kinases and phosphatases (e.g. MEK and PP2A), acetylases and deacetylases (e.g. SIRT1 and EP300), and transcriptional co-regulators (e.g. ATF1 and Strap) modulate HSF1-mediated gene expression (Asano et al., 2016; Ishikawa et al., 2015; Raychaudhuri et al., 2014; Takii et al., 2015; Tang et al., 2015; Westerheide et al., 2009; Xu et al., 2008), it will be interesting to study the effects of physiological factors that affect these modulators on HDIS. Finally, our data suggest that DHRS2 is an important mediator of cellular senescence. *DHRS2* gene expression is activated by oxidative stress-sensitive transcriptional factors, including nuclear factor erythroid 2-related factor (NRF2) and the ETS translocation variant 5 (ETV5) (Crean et al., 2012; Monge et al., 2009). It is important to clarify the role of the DHRS2-MDM2-p53 pathway in cellular senescence induced by oxidative stress.

MATERIALS AND METHODS

Plasmids

Tet-pLKO-neo (plasmid #21916) and p1322 HPV16 E6 (plasmid #8642) were obtained from Addgene (Cambridge, MA). pLKO.1-puro was purchased from Sigma (St. Louis, MO). pLKO.1-blast was constructed by replacing the puromycin resistance gene in pLKO.1-puro with a blasticidin S resistance gene. CSII-CMV-MCS-IRES2-Bsd, pCAG-HIVgp, and pCMV-VSV-G-RSV-Rev plasmids were kindly provided by Dr H. Miyoshi (RIKEN BioResource Center, Ibaraki, Japan). Tet-pLKO-neo-shHSF1, pLKO.1-puro-shGFP, pLKO.1-puro-shHSF1, pLKO.1-blast-shGFP, pLKO.1-blast-shHSF1, pLKO.1-blast-shHSF1 #2, pLKO.1-blast-shHSF2, pLKO.1-blast-shp53, pLKO.1-blast-shp21, and pLKO.1-blast-shDHRS2 #1, #2 plasmids were constructed by inserting the annealed oligonucleotides corresponding to target sequences into pLKO plasmids. Target sequences are shown in Table S1. HSF1 K80Q mutant was generated by using the QuikChange II Site-Directed Mutagenesis kit (Agilent Technologies, Santa Clara, CA). HSF1 Δ156–226 and Δ454–529 mutants were generated by PCR. The HSF1 R71G mutant was described previously (Inouye et al., 2003). cDNAs encoding WT-HSF1 or K80Q, R71G, Δ156–226, and Δ454–529 mutants HSF1 were subcloned into CSII-CMV-MCS-IRES2-Bsd.

Lentivirus preparation

HEK293T cells were cultured in Dulbecco's modified Eagle's medium (DMEM) (Wako, Osaka, Japan) containing 10% fetal bovine serum (FBS) at 37°C under 5% CO_2. Cells were seeded in a collagen type I-coated dish (IWAKI, Shizuoka, Japan) 18–24 h before transfection at a density of 1–2×10^5 cells/cm^2. The pLKO plasmids or the CMII-CMV-MCS-IRES2-Bsd plasmids were co-transfected with pCAG-HIVgp and pCMV-VSV-G-RSV-Rev into HEK293T cells at a ratio of 2:1:1 using Lipofectamine 2000 Transfection Reagent (Thermo Fisher Scientific, Waltham, MA) to produce lentivirus vectors. Forty-eight to 72 h after transfection, recombinant lentivirus-containing supernatants were collected.

Cell culture and reagents

Normal human diploid fibroblasts (HDFs), such as cell lines MRC-5, TIG-1 and TIG-3, and the hTERT-immortalized HDF cell line (OUMS-36T-3F) were purchased from JCRB Cell Bank (Tokyo, Japan). Human osteosarcoma (U2OS, ATCC) cells were authenticated but human adenocarcinoma (MCF7, ATCC) cells were not. All cells were confirmed as mycoplasma-free by using the 4′6-diamidino-2-phenylindole (DAPI) (DAPI Fluoromount-G, SouthernBiotech, Birmingham, AL) method and maintained in DMEM containing 10% FBS at 37°C under 5% CO_2. OUMS/Tet-on shHSF1 cells were obtained by infection with the recombinant lentiviral vector Tet-pLKO-neo-shHSF1. Infected OUMS-36T-3F cells were selected in 1 mg/ml G418 (Wako) and cloned. OUMS/Tet-on shHSF1 cells stably expressing WT or mutant HSF1 were obtained by using recombinant lentiviral vectors CSII-CMV-MCS-IRES2-Bsd corresponding to HSF1 cDNAs. Infected OUMS/Tet-on shHSF1 cells were selected in 40 µg/ml blasticidin S (Wako). OUMS/Tet-on shHSF1 cells stably expressing HPV16 E6 were obtained by co-transfection of a plasmid harboring a hygromycin resistance gene and p1322 HPV16 E6 at a ratio of 1:9 by using FuGENE6 (Promega, Madison, WI). Transfected cells were selected in 0.2 mg/ml hygromycin B (Wako) and cloned. OUMS/Tet-on shHSF1 cells stably expressing shRNAs targeting GFP, p53, p21 or DHRS2 were obtained using recombinant lentiviral vectors pLKO.1-blast-shGFP, -shp53, -shp21 or -shDHRS2, respectively. Infected cells were selected in blasticidin S as described above. DOX (Sigma) was used at a concentration of 1 µg/ml. CHX (Sigma), Nutlin-3 (Santa Cruz Biotechnology, Santa Cruz, CA) and SB203580 (Wako) were used at a concentration of 100 µg/ml, 10 µM and 20 µM, respectively. MG132 (Sigma), 17-AAG (Wako), H_2O_2 (Wako) and VER155008 (Sigma) were used at the indicated concentrations.

Antibodies

Rabbit polyclonal antiserum against DHRS2 was generated by Eurofins Genomics (Tokyo, Japan). Two synthetic peptides (QQNVDRAMAKLQGE and CHVGKAEDREQLVAK) were used to immunize rabbits. Other antibodies used in this study are listed in Table S2.

IdU and BrdU incorporation assay

Cells cultured in 12-well plates were pulse-labeled with 10 µM 5-iodo-2′-deoxyuridine (IdU, Sigma) for 30 min and washed once with PBS. After fixation with 70% ethanol at −30°C overnight, cells were incubated with 2.5 N HCl for 30 min at room temperature (RT), followed by incubation with 0.1 M $Na_2B_4O_7$ for 10 min at RT. Then, cells were incubated for 30 min in blocking buffer [PBS containing 10% normal goat serum, 3% bovine serum albumin, and 0.1% Nonidet P40 (NP40)], followed by incubation in blocking buffer containing anti-IdU/anti-5-Bromo-2′-deoxyuridine (BrdU) antibody, (BD Bioscience, Franklin Lake, NJ) for 2 h at RT. Cells were washed with washing buffer (PBS containing 0.1% NP40) three times and incubated with anti-mouse IgG antibody conjugated to Alexa-Fluor-555 (Thermo Fisher Scientific) for 1 h at RT in the dark. After washing cells, nuclei were counterstained with DAPI. Similarly, BrdU-labeled cells were detected by anti-BrdU antibody. Images were obtained using a fluorescence microscope [DM IRB (Leica, Wetzlar, Germany), with a LEICA DFC3000 G camera, a 20× N Plan L 0.35-NA objective lens, and Leica Application Suite software]. More than 200 cells were counted to determine the percentage of labeled cells.

SA-β-gal assay

The SA-β-gal assay was performed as described previously (Dimri et al., 1995). Briefly, cells were washed with PBS, fixed with 3.7% formaldehyde in PBS for 5 min at RT and washed with PBS twice. Cells were stained by incubation with SA-β-gal-staining solution [1 mg/ml 5-bromo-4-chloro-3-indolyl-β-D-galactoside, 5 mM $K_3Fe(CN)_6$, 5 mM $K_4Fe(CN)_6$, 2 mM $MgCl_2$, 150 mM NaCl, 20 mM citric acid, 40 mM Na_2HPO_4, pH 6.0] overnight at 37°C. Nuclei were counterstained with KARYOMAX Giemsa

stain improved R66 solution (Invitrogen, Carlsbad, CA). Images were obtained using an OLYMPUS IX70 microscope (Olympus, Tokyo, Japan) with a digital camera. More than 200 cells were counted to determine the percentage of SA-β-gal-positive cells.

SAHF analysis

To detect formation of senescence-associated heterochromatin foci (SAHF), cells were washed with PBS and fixed with 3.7% formaldehyde in PBS for 5 min at RT. Subsequently, cells were washed once with PBS and incubated with 0.3% Triton X-100 in PBS for 10 min at RT. Nuclei were stained with 1 µg/ml of DAPI for 30 min, followed by washing with PBS twice. Images were obtained using fluorescence microscope (DM IRB, with a LEICA DFC3000 G camera, a 40× N Plan L 0.55-NA objective lens, and Leica Application Suite software). More than 200 cells were counted to determine the percentage of SAHF-positive cells.

qPCR and data analysis

Total RNA was prepared using RNeasy Mini kit (Qiagen, Hilden, Germany) and cDNA was synthesized from 1–2 µg total RNA using a cDNA synthesis kit (FSQ-101, Toyobo, Tokyo, Japan) according to the manufacturer's protocol. Then, cDNA was subjected to qPCR using pre-designed gene-specific primers and probe sets (PrimeTime Std qPCR Assay, IDT, Coralville, IA) and a reaction mixture (QPS-101, Toyobo). The sequences of primers and probes for genes are shown in Table S3. GAPDH was used as a reference gene. Accumulation of PCR products was monitored in real time by measuring the level of fluorescence (PikoReal 96 Real-Time PCR System, Thermo Fisher Scientific). Results were analyzed by the $\Delta\Delta C_t$ methods and normalized to *GAPDH* using PikoReal software (Thermo Fisher Scientific) to determine relative fold-changes of gene expression.

Immunoblotting

Cells were washed with cold PBS once and directly lysed in Laemmli sample buffer [62.5 mM Tris pH 6.8, 2% sodium dodecyl sulfate (SDS), 20% glycerol]. Cell lysates were sonicated with a Branson Sonifier 150 (Branson Ultrasonics, Danbury, CT) at setting 4 with 10 s pulses three times. After determining the protein concentration of each sample, 2-mercaptoethanol and Bromophenol Blue were added to the lysates at the concentrations of 5% and 0.025%, respectively. Then, the lysates were boiled for 7 min and used as whole-cell lysates (WCLs). Equal amounts of protein (3–7 µg) were subjected to electrophoresis using a 5–20% polyacrylamide gradient gel (e-PAGEL, ATTO, Tokyo, Japan). The electrophoretically separated proteins were transferred to polyvinylidene difluoride membranes (Pall Corporation, Dreieich, Germany) using a submarine transfer apparatus (Criterion Blotter, BioRad, Hercules, CA). Immunoblotting was performed using standard procedures. Protein signals were densitometrically quantified using National Institutes of Health Image software (ImageJ). The area of blot was enclosed, and the integrated intensity was calculated using the following formula: area×(mean intensity−background).

Immunostaining

Cells cultured in 12-well plates were washed with PBS once and fixed with 3.7% formaldehyde in PBS for 20 min, followed by permeabilization with 0.3% Triton X-100 in PBS for 15 min at RT. Then, cells were incubated for 30 min in blocking buffer, followed by incubation in blocking buffer containing the primary antibody for 2 h at RT. Cells were washed with washing buffer three times and incubated with a secondary antibody conjugated to Alexa-Fluor-488 or Alexa-Fluor-555 in the dark for 1 h at RT. Cells were washed as described above and nuclei were counterstained with DAPI. In case of double staining for SA-β-gal and HSPA1A, cells were first assayed for SA-β-gal, followed by immunostaining for HSPA1A.

Immunoprecipitation

To detect polyubiquitylated p53, cells were washed once with cold PBS, followed by lysis in RIPA buffer (50 mM Tris pH 7.5, 150 mM NaCl, 1% NP40, 0.5% sodium deoxycholate, 0.1% SDS). Cell lysates were collected in 1.5 ml centrifuge tubes and sonicated with a Branson Sonifier 150 at setting 4 with 10 s pulses three times. Then, cell lysates were centrifuged for 10 min at 16,000 ***g*** and supernatants were immunoprecipitated with rabbit polyclonal anti-p53 antibody (2 µg) followed by immunoblotting. To detect the interaction between DHRS2 and MDM2, U2OS cells were lysed in RIPA buffer and lysates were centrifuged as described above; supernatants were then immunoprecipitated with 3 µl of pre-immune serum or anti-DHRS2 serum followed by immunoblotting.

FACS analysis

Cells were trypsinized and collected in a centrifuge tube. Then, cells were washed once with cold PBS, followed by fixing with 70% ethanol at −30°C overnight. After removing ethanol, cells were permeabilized in 0.3% Triton X-100 in PBS for 5 min at RT, then suspended in propidium iodide staining solution [PBS containing 25 µg/ml propidium iodide (Sigma) and 10 µg/ml RNase A (Sigma)] in the dark for 2 h at RT. BD FACSVerse was used to measure the signals of forward scatter and side scatter, and DNA contents. Data were analyzed using FlowJo software (Tree Star, Ashland, OR).

Microarray analysis

Total RNA was isolated using an RNeasy Mini kit. Labeled RNA generated using a Low Input Quick Amp labeling kit (Agilent Technologies) were fragmented and hybridized to Sureprint G3 Human Gene Expression 8×60k (Agilent Technologies). After washing, the arrays were scanned with an Agilent microarray scanner G2539A (Agilent Technologies). Data were analyzed using GeneSpring GX version 11.5 (Agilent Technologies). Microarray expression profiling was performed by Oncomics (Nagoya, Japan).

ChIP assay

OUMS/Tet-on shHSF1 cells were incubated with vehicle or DOX for 3 days, and a ChIP assay was performed using SimpleChIP Enzymatic Chromatin IP kit (Cell Signaling Technology, Beverly, MA), according to the manufacturer's protocol. Chromatin prepared from ∼5×10^6 cells was immunoprecipitated with anti-HSF1 antibody (Cell Signaling Technology) or control rabbit IgG. Chromatin prepared from OUMS/Tet-on shHSF1 cells transduced with WT-HSF1 or empty vector was immunoprecipitated as described above. qPCR of ChIP-enriched DNAs was performed using the primers listed in Table S4 and LightCycler 480 SYBR Green I master mix (Roche Diagnostics, Mannheim, Germany). Percentage input was determined by comparing the cycle threshold value of each sample to a standard curve generated using a 4-point, 10-fold serial dilution of input.

Statistical analysis

Statistical analyses were performed using two-tailed Student's *t*-test unless otherwise indicated. Data are presented as the mean±standard deviation (s.d.). Values of $P<0.05$ were considered significant.

Acknowledgements

We thank K. Tomizawa for technical help and H. Miyoshi for generous gifts of materials. We also thank Michal Bell Ph.D. and J. Ludovic Croxford Ph.D. from Edanz (www.edanzediting.com/ac) for editing a draft of this manuscript.

Competing interests

The authors declare no competing or financial interests.

Author contributions

Conceptualization: T.O., M.F., A.N., T.Y.; Methodology: T.O., M.F.; Investigation: T.S., K.K.; Resources: M.F., A.N.; Writing - original draft: T.O., T.Y.; Writing - review & editing: T.O., T.S., K.K., T.Y.; Supervision: A.N., T.Y.; Funding acquisition: T.O.

Funding

This work was supported by the Japan Society for the Promotion of Science (JSPS) KAKENHI [Grant number JP15K06866 to T.O.]. Financial support was also provided by the Takeda Science Foundation and the Osaka Cancer Research Foundation.

Data availability

Microarray data from this study have been deposited in the NCBI Gene Expression Omnibus (GEO) database with accession number GSE111355.

Supplementary information

Supplementary information available online at
http://jcs.biologists.org/lookup/doi/10.1242/jcs.210724.supplemental

References

Abbas, T. and Dutta, A. (2009). p21 in cancer: intricate networks and multiple activities. *Nat. Rev. Cancer* **9**, 400-414.

Anckar, J. and Sistonen, L. (2011). Regulation of HSF1 function in the heat stress response: implications in aging and disease. *Annu. Rev. Biochem.* **80**, 1089-1115.

Asano, Y., Kawase, T., Okabe, A., Tsutsumi, S., Ichikawa, H., Tatebe, S., Kitabayashi, I., Tashiro, F., Namiki, H., Kondo, T. et al. (2016). IER5 generates a novel hypo-phosphorylated active form of HSF1 and contributes to tumorigenesis. *Sci. Rep.* **6**, 19174.

Baker, D. J., Wijshake, T., Tchkonia, T., LeBrasseur, N. K., Childs, B. G., van de Sluis, B., Kirkland, J. L. and van Deursen, J. M. (2011). Clearance of p16Ink4a-positive senescent cells delays ageing-associated disorders. *Nature* **479**, 232-236.

Baker, D. J., Childs, B. G., Durik, M., Wijers, M. E., Sieben, C. J., Zhong, J., Saltness, R. A., Jeganathan, K. B., Verzosa, G. C., Pezeshki, A. et al. (2016). Naturally occurring p16(Ink4a)-positive cells shorten healthy lifespan. *Nature* **530**, 184-189.

Bieging, K. T., Mello, S. S. and Attardi, L. D. (2014). Unravelling mechanisms of p53-mediated tumour suppression. *Nat. Rev. Cancer* **14**, 359-370.

Campisi, J. (2013). Aging, cellular senescence, and cancer. *Annu. Rev. Physiol.* **75**, 685-705.

Crean, D., Felice, L., Taylor, C. T., Rabb, H., Jennings, P. and Leonard, M. O. (2012). Glucose reintroduction triggers the activation of Nrf2 during experimental ischemia reperfusion. *Mol. Cell. Biochem.* **366**, 231-238.

Dai, C., Whitesell, L., Rogers, A. B. and Lindquist, S. (2007). Heat shock factor 1 is a powerful multifaceted modifier of carcinogenesis. *Cell* **130**, 1005-1018.

Deisenroth, C., Thorner, A. R., Enomoto, T., Perou, C. M. and Zhang, Y. (2010). Mitochondrial Hep27 is a c-Myb target gene that inhibits Mdm2 and stabilizes p53. *Mol. Cell. Biol.* **30**, 3981-3993.

Dimri, G. P., Lee, X., Basile, G., Acosta, M., Scott, G., Roskelley, C., Medrano, E. E., Linskens, M., Rubelj, I., Pereira-Smith, O. et al. (1995). A biomarker that identifies senescent human cells in culture and in aging skin in vivo. *Proc. Natl. Acad. Sci. USA* **92**, 9363-9367.

Duensing, S. and Münger, K. (2004). Mechanisms of genomic instability in human cancer: insights from studies with human papillomavirus oncoproteins. *Int. J. Cancer* **109**, 157-162.

El-Brolosy, M. A. and Stainier, D. Y. R. (2017). Genetic compensation: a phenomenon in search of mechanisms. *PLoS Genet.* **13**, e1006780.

Fåhraeus, R. and Olivares-Illana, V. (2014). MDM2's social network. *Oncogene* **33**, 4365-4376.

Fujimoto, M., Takaki, E., Takii, R., Tan, K., Prakasam, R., Hayashida, N., Iemura, S., Natsume, T. and Nakai, A. (2012). RPA assists HSF1 access to nucleosomal DNA by recruiting histone chaperone FACT. *Mol. Cell* **48**, 182-194.

Gabai, V. L., Yaglom, J. A., Waldman, T. and Sherman, M. Y. (2009). Heat shock protein Hsp72 controls oncogene-induced senescence pathways in cancer cells. *Mol. Cell. Biol.* **29**, 559-569.

Gomez-Pastor, R., Burchfiel, E. T. and Thiele, D. J. (2017). Regulation of heat shock transcription factors and their roles in physiology and disease. *Nat. Rev. Mol. Cell Biol.* **19**, 4-19.

Guertin, M. J. and Lis, J. T. (2010). Chromatin landscape dictates HSF binding to target DNA elements. *PLoS Genet.* **6**, e1001114.

Hahn, J.-S., Hu, Z., Thiele, D. J. and Iyer, V. R. (2004). Genome-wide analysis of the biology of stress responses through heat shock transcription factor. *Mol. Cell. Biol.* **24**, 5249-5256.

Hayashida, N., Fujimoto, M., Tan, K., Prakasam, R., Shinkawa, T., Li, L., Ichikawa, H., Takii, R. and Nakai, A. (2010). Heat shock factor 1 ameliorates proteotoxicity in cooperation with the transcription factor NFAT. *EMBO J.* **29**, 3459-3469.

He, S. and Sharpless, N. E. (2017). Senescence in health and disease. *Cell* **169**, 1000-1011.

Hensen, S. M. M., Heldens, L., van Genesen, S. T., Pruijn, G. J. M. and Lubsen, N. H. (2013). A delayed antioxidant response in heat-stressed cells expressing a non-DNA binding HSF1 mutant. *Cell Stress Chaperones* **18**, 455-473.

Hoffman, Y., Pilpel, Y. and Oren, M. (2014). microRNAs and Alu elements in the p53-Mdm2-Mdm4 regulatory network. *J. Mol. Cell Biol.* **6**, 192-197.

Inouye, S., Katsuki, K., Izu, H., Fujimoto, M., Sugahara, K., Yamada, S., Shinkai, Y., Oka, Y., Katoh, Y. and Nakai, A. (2003). Activation of heat shock genes is not necessary for protection by heat shock transcription factor 1 against cell death due to a single exposure to high temperatures. *Mol. Cell. Biol.* **23**, 5882-5895.

Ishikawa, Y., Kawabata, S. and Sakurai, H. (2015). HSF1 transcriptional activity is modulated by IER5 and PP2A/B55. *FEBS Lett.* **589**, 1150-1155.

Kim, G., Meriin, A. B., Gabai, V. L., Christians, E., Benjamin, I., Wilson, A., Wolozin, B. and Sherman, M. Y. (2012). The heat shock transcription factor Hsf1 is downregulated in DNA damage-associated senescence, contributing to the maintenance of senescence phenotype. *Aging Cell* **11**, 617-627.

Kruse, J.-P. and Gu, W. (2009). Modes of p53 regulation. *Cell* **137**, 609-622.

Labbadia, J. and Morimoto, R. I. (2015). The biology of proteostasis in aging and disease. *Annu. Rev. Biochem.* **84**, 435-464.

Lee, Y. J., Lee, H. J., Lee, J. S., Jeoung, D., Kang, C. M., Bae, S., Lee, S. J., Kwon, S. H., Kang, D. and Lee, Y. S. (2008). A novel function for HSF1-induced mitotic exit failure and genomic instability through direct interaction between HSF1 and Cdc20. *Oncogene* **27**, 2999-3009.

Li, J. and Kurokawa, M. (2015). Regulation of MDM2 stability after DNA damage. *J. Cell. Physiol.* **230**, 2318-2327.

Manfredi, J. J. (2010). The Mdm2-p53 relationship evolves: Mdm2 swings both ways as an oncogene and a tumor suppressor. *Genes Dev.* **24**, 1580-1589.

Massey, A. J., Williamson, D. S., Browne, H., Murray, J. B., Dokurno, P., Shaw, T., Macias, A. T., Daniels, Z., Geoffroy, S., Dopson, M. et al. (2010). A novel, small molecule inhibitor of Hsc70/Hsp70 potentiates Hsp90 inhibitor induced apoptosis in HCT116 colon carcinoma cells. *Cancer Chemother. Pharmacol.* **66**, 535-545.

Mendillo, M. L., Santagata, S., Koeva, M., Bell, G. W., Hu, R., Tamimi, R. M., Fraenkel, E., Ince, T. A., Whitesell, L. and Lindquist, S. (2012). HSF1 drives a transcriptional program distinct from heat shock to support highly malignant human cancers. *Cell* **150**, 549-562.

Meng, L., Gabai, V. L. and Sherman, M. Y. (2010). Heat-shock transcription factor HSF1 has a critical role in human epidermal growth factor receptor-2-induced cellular transformation and tumorigenesis. *Oncogene* **29**, 5204-5213.

Meng, L., Hunt, C., Yaglom, J. A., Gabai, V. L. and Sherman, M. Y. (2011). Heat shock protein Hsp72 plays an essential role in Her2-induced mammary tumorigenesis. *Oncogene* **30**, 2836-2845.

Min, J.-N., Huang, L., Zimonjic, D. B., Moskophidis, D. and Mivechi, N. F. (2007). Selective suppression of lymphomas by functional loss of Hsf1 in a p53-deficient mouse model for spontaneous tumors. *Oncogene* **26**, 5086-5097.

Monge, M., Colas, E., Doll, A., Gil-Moreno, A., Castellvi, J., Diaz, B., Gonzalez, M., Lopez-Lopez, R., Xercavins, J., Carreras, R. et al. (2009). Proteomic approach to ETV5 during endometrial carcinoma invasion reveals a link to oxidative stress. *Carcinogenesis* **30**, 1288-1297.

Muñoz-Espín, D. and Serrano, M. (2014). Cellular senescence: from physiology to pathology. *Nat. Rev. Mol. Cell. Biol.* **15**, 482-496.

O'Callaghan-Sunol, C., Gabai, V. L. and Sherman, M. Y. (2007). Hsp27 modulates p53 signaling and suppresses cellular senescence. *Cancer Res.* **67**, 11779-11788.

Östling, P., Björk, J. K., Roos-Mattjus, P., Mezger, V. and Sistonen, L. (2007). Heat shock factor 2 (HSF2) contributes to inducible expression of hsp genes through interplay with HSF1. *J. Biol. Chem.* **282**, 7077-7086.

Ragazzon, B., Libe, R., Gaujoux, S., Assie, G., Fratticci, A., Launay, P., Clauser, E., Bertagna, X., Tissier, F., de Reynies, A. et al. (2010). Transcriptome analysis reveals that p53 and {beta}-catenin alterations occur in a group of aggressive adrenocortical cancers. *Cancer Res.* **70**, 8276-8281.

Raychaudhuri, S., Loew, C., Körner, R., Pinkert, S., Theis, M., Hayer-Hartl, M., Buchholz, F. and Hartl, F. U. (2014). Interplay of acetyltransferase EP300 and the proteasome system in regulating heat shock transcription factor 1. *Cell* **156**, 975-985.

Rohde, M., Daugaard, M., Jensen, M. H., Helin, K., Nylandsted, J. and Jaattela, M. (2005). Members of the heat-shock protein 70 family promote cancer cell growth by distinct mechanisms. *Genes Dev.* **19**, 570-582.

Solís, E. J., Pandey, J. P., Zheng, X., Jin, D. X., Gupta, P. B., Airoldi, E. M., Pincus, D. and Denic, V. (2016). Defining the essential function of yeast Hsf1 reveals a compact transcriptional program for maintaining eukaryotic proteostasis. *Mol. Cell* **63**, 60-71.

Su, K.-H., Cao, J., Tang, Z., Dai, S., He, Y., Sampson, S. B., Benjamin, I. J. and Dai, C. (2016). HSF1 critically attunes proteotoxic stress sensing by mTORC1 to combat stress and promote growth. *Nat. Cell Biol.* **18**, 527-539.

Sugrue, M. M., Shin, D. Y., Lee, S. W. and Aaronson, S. A. (1997). Wild-type p53 triggers a rapid senescence program in human tumor cells lacking functional p53. *Proc. Natl. Acad. Sci. USA* **94**, 9648-9653.

Takii, R., Fujimoto, M., Tan, K., Takaki, E., Hayashida, N., Nakato, R., Shirahige, K. and Nakai, A. (2015). ATF1 modulates the heat shock response by regulating the stress-inducible heat shock factor 1 transcription complex. *Mol. Cell. Biol.* **35**, 11-25.

Tang, Z., Dai, S., He, Y., Doty, R. A., Shultz, L. D., Sampson, S. B. and Dai, C. (2015). MEK guards proteome stability and inhibits tumor-suppressive amyloidogenesis via HSF1. *Cell* **160**, 729-744.

Trinklein, N. D., Murray, J. I., Hartman, S. J., Botstein, D. and Myers, R. M. (2004). The role of heat shock transcription factor 1 in the genome-wide regulation of the mammalian heat shock response. *Mol. Biol. Cell* **15**, 1254-1261.

Verma, P., Pfister, J. A., Mallick, S. and D'Mello, S. R. (2014). HSF1 protects neurons through a novel trimerization- and HSP-independent mechanism. *J. Neurosci.* **34**, 1599-1612.

Wade, M., Li, Y.-C. and Wahl, G. M. (2013). MDM2, MDMX and p53 in oncogenesis and cancer therapy. *Nat. Rev. Cancer* **13**, 83-96.

Wang, J.-H., Yao, M.-Z., Gu, J.-F., Sun, L.-Y., Shen, Y.-F. and Liu, X.-Y. (2002). Blocking HSF1 by dominant-negative mutant to sensitize tumor cells to hyperthermia. *Biochem. Biophys. Res. Commun.* **290**, 1454-1461.

Warfel, N. A. and El-Deiry, W. S. (2013). p21WAF1 and tumourigenesis: 20 years after. *Curr. Opin. Oncol.* **25**, 52-58.

Westerheide, S. D., Anckar, J., Stevens, S. M., Jr, Sistonen, L. and Morimoto, R. I. (2009). Stress-inducible regulation of heat shock factor 1 by the deacetylase SIRT1. *Science* **323**, 1063-1066.

Xu, D., Zalmas, L. P. and La Thangue, N. B. (2008). A transcription cofactor required for the heat-shock response. *EMBO Rep.* **9**, 662-669.